Regional frequency analysis of heavy precipitation totals in the High Tatras region in Slovakia for flood risk estimation

L. Gaál, J. Szolgay
Faculty of Civil Engineering, Slovak University of Technology[1]

M. Lapin
Faculty of Mathematics, Physics and Informatics, Comenius University[2]

A b s t r a c t : Regional frequency analysis of heavy precipitation totals based on the estimation of parameters of the distribution function using L-moments has recently been adopted in the geographical-climatological conditions of Slovakia. On the basis of the most reliable records of daily precipitation totals from 56 climatological stations from the whole country, 3 homogeneous regions have been delineated for the purposes of the regional frequency analysis of 1 to 5-day precipitation maxima in warm/cold seasons, and the calendar year, respectively *(Gaál, 2006)*. The recent study focuses on one of these regions consisting of 16 stations that also encompasses the whole High Tatras region. The paper as a case study presents a complete procedure of the estimation of the design precipitation along with the estimation of their uncertainty bounds.

Key words: regional frequency analysis, heavy 1 to 5-day precipitation totals, design values, homogeneity tests, goodness-of-fit tests, High Tatras, Slovakia

1. Introduction

The incidence of several major flood events in Slovakia over the past decade has also led to concerns about the level of reliability provided by existing flood warning systems. The need to better quantify the severity of

[1] Radlinského 11, 813 68 Bratislava, Slovak Republic
e-mail: ladislav.gaal@stuba.sk; jan.szolgay@stuba.sk
[2] Mlynská dolina, F1, 842 48 Bratislava, Slovak Republic
e-mail: lapin@fmph.uniba.sk

forthcoming events in order to introduce reliable pre-flood warnings became evident. When an extreme meteorological situation that can lead to a flood causing major disruption, damage and possibly loss of life is approaching a basin, one of the key questions that should be posed is how dangerous the flood that can be expected to occur may be. Warnings based emergency planning could profit from an estimate of the return periods of the expected flood. A case study-based development of such a method on the Hron and Torysa Rivers was presented in *Hlavčová et al. (2005)*. In that approach modelled real time data on the soil moisture conditions in a catchment in conjunction with estimates of the extremity of the future rainfall were used in a scenario-based method. Implementation of the method relied on the regional frequency analysis of annual maxima of 1 to 5-day precipitation totals.

Such an analysis is also of interest for the estimation of the return periods of rare precipitation events in ex-post flood analysis (*Norbiato et al., 2007*). As they noted, due to the scarcity of discharge data, reliable regional rainfall frequency estimates are needed to describe the characteristics of a rare flood event.

In ex-post flood analysis, often the return period of the greatest point rainfall intensity observed during a storm event is taken as the return period of the whole storm (*Ramos et al., 2005*). When radar observations, which have large potential to improve the description of the flood generating precipitation, and therefore may be used for flood and flash flood analysis (see e.g. *Borga, 2002; Gaume et al., 2004; Delrieu et al., 2005*) are missing, regional frequency analysis may be used to reduce the uncertainty in the assessment of return periods for extreme flood and flash flood-producing rainfall for various rainfall durations (*Norbiato et al., 2007*).

A review of case studies and rainfall frequency studies undertaken by national meteorological offices in several countries (see e.g. *Hlavčová et al., 2005; Wallis et al., 2007*) showed that methods for regional frequency analysis have undergone rapid development in the recent past. Studies in Switzerland, the State of Washington, Germany (the large research project known as KOSTRA), in the UK (the Flood Estimation Handbook), New Zealand (The High Intensity Rainfall Design System - HIRDS) and South Africa showed that, in practice, attention has been paid also to the analysis of precipitation with a duration longer than 24 hours and that the spatial

distribution of precipitation was increasingly analyzed. Methods based on L-moments and the use of the generalized extreme value (GEV) probability distribution function seemed to gain increased popularity in recent years.

This paper is a case study based description of such an up-to-date regional frequency analysis methodology applied to precipitation data of durations of one to five days over the High Core Mountain region of Slovakia. The paper reviews the main items of the L-moments based regional frequency analysis algorithm of *Hosking and Wallis (1997)* and describes the extreme precipitation regime of the High Core Mountains of Slovakia.

2. Methods

2.1. General concepts

The L-moments based regional frequency analysis (abbr. RFA) of *Hosking and Wallis (1997)* has been adopted to estimate the design precipitation in Slovakia.

L-moments are an alternative tool for describing scale and shape statistics of a data sample or a probability distribution (location, scale, skewness, kurtosis etc.). The prefix L denotes the fact that these statistics are computed from the linear combination of the data sample sorted in ascending order. L-moments are superior to the conventional moments in a lot of aspects: e.g. they are more robust to the presence of outliers; they do not have sample size related bounds or are less subject to bias in estimation (*Hosking, 1990; Vogel and Fenessey, 1993; Sankarasubramanian and Srinivasan, 1999*). For the definition formulae of the L-moments and an overview of their statistical properties, see *Hosking (1990)* or *Hosking and Wallis (1997)*.

The *index value method* (*Dalrymple, 1960*) is a technique for pooling information from different data samples. Recently, it is the most frequently used methodology in the regional approach to a frequency analysis of extraordinary events in environmental sciences. The index value method supposes that the proposed group of similar sites forms a homogeneous region; that is, sites pooled together exhibit, except for a scaling factor, similar probability distribution curves (growth curves) of extremes. In a mathematical form:

$$X_T^{(i)} = \mu^{(i)} x_T, \quad i = 1, \ ..., \ N, \tag{1}$$

where i denotes the site of the interest, N is the total number of the sites in the region, $X_T^{(i)}$ the at-site design value corresponding to the return period T, x_T is the dimensionless regional T-year quantile, and $\mu^{(i)}$ is the *index value*, i.e. the at-site scale factor. The index value (especially termed as *index flood* in hydrology, and *index storm* in climatology, respectively) is usually estimated by the at-site sample mean of the selected variable.

Hosking and Wallis (1997) were the first who united the index value method and the toolbox of L-moments into a generally accepted guideline to a RFA. Their procedure consists of four major steps:

1. screening of the data;
2. identification of homogeneous regions;
3. choice of a frequency distribution;
4. estimation of the regional frequency distribution, at-site quantiles and their confidence intervals.

The very first step of the Hosking and Wallis's regional approach is a comprehensive scrutiny of the selected data set. Such a procedure is aimed at revealing gross errors such as outliers, repeated values, trends, shift changes or other irregularities in the data sample. Due to the fact that the screening of the data is an inherent part of any climatological analysis, we will not deal with it in details; instead, the last three items of the list above will be discussed more thoroughly.

2.2. Identification of the regions and assessing their homogeneity

The identification of homogeneous regions is a crucial problem of the RFA. The aim of this procedure is to find groups of sites with identical frequency distributions except for a site-specific scale factor. There are plenty of statistical techniques (e.g. cluster analysis, principal component analysis etc.) how to form groups of similar sites, however, the final composition of regions is usually affected by subjective considerations, mostly depending on the researcher's knowledge about the climatological-geographical peculiarities of the target areas.

In order to assess whether the composition of physically plausible regions are meaningful homogeneity tests are used. The most powerful ones, according to a comparison of *Fill and Stedinger (1995)* are the H-test of *Hosking and Wallis (1997)* and the $X10$-test of *Lu and Stedinger (1992)*; therefore, these two tests are applied for evaluating the homogeneity of the proposed regions in the RFA of heavy precipitation totals in Slovakia.

Let us suppose that a region consists of N sites; the i-th of them is characterized by n_i (record length), $t^{(i)}$ (sample L-Cv), $t_3^{(i)}$ (sample L-skewness, L-Cs) and $t_4^{(i)}$ (sample L-kurtosis, L-Ck).

The H-test by Hosking and Wallis

The H-test measures the between-site variation of sample L-Cv-s within the actual region, and compares it with the variation that would be expected in the case of a homogeneous region. The latter, hypothetical case ('what would be expected') is determined by a simulation procedure. The test is based on the weighted standard deviation V of the at-site sample L-Cv-s:

$$V = \sqrt{\sum_{i=1}^{N} n_i \left(t^{(i)} - t^R\right)^2 \Big/ \sum_{i=1}^{N} n_i}, \tag{2}$$

where

$$t^R = \sum_{i=1}^{N} n_i t^{(i)} \Big/ \sum_{i=1}^{N} n_i \tag{3}$$

is the weighted regional average of the sample L-Cv-s with the weights proportional to the site's record length n_i. The heterogeneity measure is then

$$H = \frac{V - \mu_V}{\sigma_V}, \tag{4}$$

where the mean (standard deviation) μ_V (σ_V) of the characteristic V are obtained by a larger number (500) of Monte Carlo-simulations, according to the following scheme:

- in each simulation loop, 'artificial worlds' with the same N and n_i, $i = 1,\ldots, N$ as in the 'real world' are created;

- at each site of the region, a 4-parameter kappa distribution is fitted with parameters that correspond to the regional average of sample L-moment ratios $[1, t^R, t_3^R, t_4^R]$;
- for all the simulated regions, the parameter V is calculated;
- from all the simulations, μ_V and σ_V are determined.

A region is declared as *acceptably homogeneous*, if $H < 1$, *possibly heterogeneous*, if $1 \leq H < 2$ and *definitely heterogeneous*, if $H \geq 2$ *(Hosking and Wallis, 1997).*

The X10-test by Lu and Stedinger

The $X10$-test is based on the sampling variance of the normalized (dimensionless) 10-year precipitation x_{10} in a homogeneous region. It assumes that the precipitation extremes follow the *generalized extreme value* (GEV) distribution (e.g. *Coles, 2001*). According to Fill and Stedinger (1995), the quantile $x_{10}^{(i)}$ (the 10-year quantile of the growth curve of precipitation at i-th site) is estimated as follows:

$$x_{10}^{(i)} = \begin{cases} 1 + \frac{t^{(i)}}{1-2^{-k}} \left(1 - \frac{(-\ln 0.9)^k}{\Gamma(1+k)}\right) & \text{if } \; k \neq 0 \\ 1 + 2.4139 t^{(i)} & \text{if } \; k = 0 \end{cases} \tag{5}$$

where $\Gamma(\cdot)$ is the gamma function and k is the shape parameter of the GEV distribution:

$$k = 7.8590C + 2.9554C^2 \text{ and } \; C = \frac{2}{t_3^{(i)} + 3} - \frac{\ln 2}{\ln 3}. \tag{6}$$

The heterogeneity measure of the $X10$-test is then

$$\chi_R^2 = \sum_{i=1}^{N} \frac{\left(x_{10}^{(i)} - x_{10}^R\right)^2}{\mathrm{var} x_{10}^{(i)}}, \tag{7}$$

where

$$x_{10}^R = \sum_{i=1}^{N} n_i x_{10}^{(i)} \Big/ \sum_{i=1}^{N} n_i \tag{8}$$

is the weighted regional average of $x_{10}^{(i)}$, and $\mathrm{var}x_{10}^{(i)}$ is the asymptotic variance of $x_{10}^{(i)}$. The asymptotic variance is usually determined from a large number of simulations; however, *Lu and Stedinger (1992)* provide tables for $\mathrm{var}x_{10}^{(i)}$.

The test statistic χ_R^2 has approximately a chi-square distribution with N-1 degrees of freedom. If $\chi_R^2 < \chi_{0.95,N-1}^2$ the null hypothesis cannot be rejected; that is, the region may be considered as homogeneous at the confidence level 95%. In the opposite case, one will reject the null hypothesis, so the region may be regarded as heterogeneous (*Lu and Stedinger, 1992*).

2.3. Choice of the frequency distribution

The goodness-of-fit tests (abbr. GOF) are statistical tools to evaluate how closely the candidate distribution function (abbr. DF) fits the data. The traditional GOF tests such as Kolmogorov-Smirnov or the χ^2 test (*Wilks, 1995*) examine the difference between the observed and theoretical frequency of events in a reasonably selected number of bins. In a regional frequency analysis, however, it is advised to employ the GOF measure of Hosking and Wallis, termed also as the Z-test (*Hosking and Wallis, 1997*). The goodness of fit is judged by how well the L-Cs and the L-Ck of the fitted distribution match the regional average L-Cs and the L-Ck of the observed data. The GOF measure according to the Z-test is the statistic

$$Z^{DF} = \frac{\tau_4^{DF} - t_4^R + B_4}{\sigma_4}, \tag{9}$$

where DF is a tag for the candidate distribution function, τ_4^{DF} is the L-kurtosis of the candidate DF, t_4^R is the regional average L-kurtosis of the data, and B_4 (σ_4) is the bias (standard deviation) of t_4^R, obtained by a large number of Monte Carlo simulations with the 4-parameter kappa distribution (for further details please refer to *Hosking and Wallis, 1997*, p. 81). In fact, $\tau_4^{DF} - t_4^R$ is the vertical distance between the points $\left[t_3^R,\ t_4^R\right]$ and $\left[t_3^R,\ \tau_4^{DF}\right]$ on the L-moment diagrams L-Ck vs. L-Cs (cf. Section 5.3., Fig. 5).

Hosking and Wallis (1997) suggest that a distribution function is acceptable to fit the data if Z^{DF} is sufficiently close to zero. A reasonable criterion is

$$\left|Z^{DIST}\right| \leq 1.64. \tag{10}$$

2.4. Estimation of the design values and their uncertainty range

The at-site quantiles, i.e. the design values for a given return period T and for a given station are estimated by the *regional L-moments algorithm* (*Hosking and Wallis, 1997*).

Suppose that the region consists of N sites. The i-th site is characterized by its record length n_i, sample mean μ_i (*index value*) and the sample L-moments ratios $t^{(i)}$, $t_3^{(i)}$, $t_4^{(i)}$, ... The regional L-moment ratios t^R and t_r^R, $r = 3,\ 4,\ ...$, are derived from the at-site sample L-moment ratios as weighted regional averages, where weights are proportional to the sites' record length n_i (see Eq. 2 for t^R; a relationship analogous to Eq. 2 holds true for t_r^R, $r = 3,\ 4,\ ...$).

The regionally weighted L-moment ratios t^R and t_r^R, $r = 3,\ 4,\ ...$ are then used to estimate the parameters of the selected distribution function in order to get the dimensionless cumulative distribution function (*growth curve*). Finally, the precipitation quantiles for a given return period T at the i-th site of the region are obtained by multiplying the dimensionless T-year quantile x_T with the index value $\mu^{(i)}$ (Eq. 1).

Besides a point estimation of the desired quantiles, the assessment of their uncertainty is of a great importance. In Hosking and Wallis's approach to a RFA, Monte Carlo simulations are suggested to assess the accuracy of the estimated quantiles. A detailed description of the simulation algorithm is given in *Hosking and Wallis, 1997*, p. 95); here we only confine to the most important pillars of the procedure:

1. each 'simulated' region has the same number of sites N, record length at each site n_i and the L-moment ratios $\left[t^{(i)},\ t_3^{(i)},\ t_4^{(i)},\ ...\right]$ as in the 'real' world;
2. the at-site parent distribution is a DF that was selected according to the GOF test (Section 2.2.); its parameters correspond to the at-site L-moment ratios $\left[t^{(i)},\ t_3^{(i)},\ t_4^{(i)},\ ...\right]$;
3. data samples are generated, taking into the consideration the actual inter-site dependence;

4. the regional L-moments algorithm is applied to the simulated sample in order to calculate the simulated quantiles;
5. the summary statistics such as bias or the root mean square error are calculated;
6. steps 2-5 are repeated 10 000 times.

The error bounds of the quantiles are determined according to the empirical quantiles of the distribution of the quantities $\hat{q}_T^{(m)} \Big/ q_T$, where $\hat{q}_T^{(m)}$ is the estimate of the T-year quantile of the regional growth curve from the m-th loop of the Monte Carlo simulation, and q_T is the actual estimate of the T-year quantile of the regional growth curve. Then 90% of the distribution of $\hat{q}_T^{(m)} \Big/ q_T$ lies within the interval between the 5^{th} and the 95^{th} quantiles:

$$k_{0.05,\,T} \leq \frac{\hat{q}_T^{(m)}}{q_T} \leq k_{0.95,\,T}. \tag{11}$$

The upper (lower) error bound $u_T(l_T)$ of the quantile estimate q_T is then

$$u_T = q_T k_{0.95,\,T} \tag{12}$$

and

$$l_T = q_T k_{0.05,\,T}. \tag{13}$$

3. Data

56 climatological stations operated by the Slovak Hydrometeorological Institute have been chosen to conduct the frequency analysis. The selected station network covers the area of the country more or less evenly (Fig. 1). Records of daily precipitation totals are available, in general, from the period 1961-2003; however, at stations with the most reliable records, the period 1951-1960 is also included in the analysis. 29 climatological stations have complete daily records with no gap during the whole period of their observation, while the rest of the stations (27) have minor gaps in their daily rainfall records (breaks of one to several-months). The missing values in the observation series have not been replaced. The basic data set at the

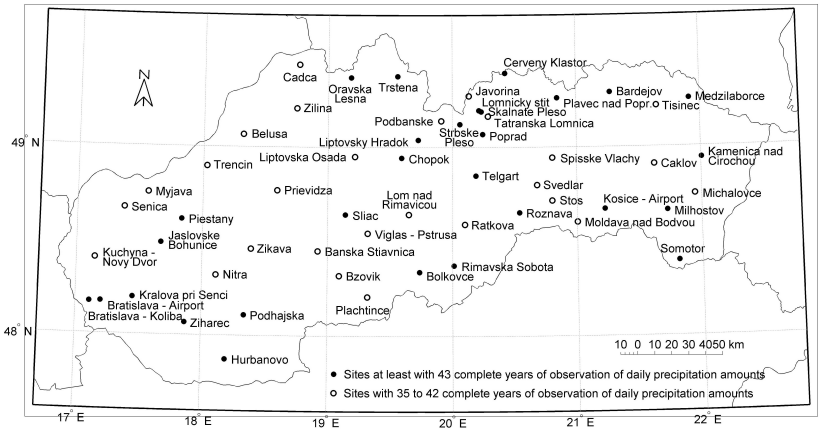

Fig. 1. 56 stations selected for a frequency analysis of heavy precipitation totals in Slovakia.

selected 56 sites makes up 2464 station-years, with the shortest (longest) observation records of length of 35 (53) years.

The k-day precipitation totals have been computed as the sums of the daily precipitation totals for k consecutive days ($k = 1, 2, 3, 4$ or 5). In the paper, different durations of the precipitation will be referred to as 1D, ..., 5D. The maxima of k-day precipitation totals have been determined for 3 seasons:

- the calendar year (labeled as Year),
- the warm season (April–September; abbr. WS), and
- the cold season (October-March; abbr. CS).

Having any missing values during a calendar year identified, annual maxima have not been determined; however, in the case of a complete season within an incomplete calendar year, the seasonal maxima have been kept for the corresponding complete season.

A standard quality checking for gross errors by means of Hosking's discordancy test *(Hosking and Wallis, 1997)* did not reveal any errors at the selected 56 stations in Slovakia. Temporal homogeneity of the observation series has been examined using several homogeneity tests. Except a single case (the highest elevated station of Lomnický štít, 2635 m a.s.l.), no signifi-

cant inhomogeneities (shift or trend changes) have been detected; therefore, the data series are regarded as sufficiently homogeneous for further climatological analyses.

4. Formation of extreme precipitation in the High Core Mountains

The region of the High Core Mountains makes up the inside of the West Carpathian belt. The High Core Mountains comprise the Eastern Tatras, the Western Tatras and the Low Tatras. The Eastern and Western Tatras are prolonged from the west to the east. The Low Tatras are elongated in an east-west direction. The Tatra Mountains are the highest mountains in Slovakia, with elevation rising from 800 to more than 2500 m above sea level. The long-term mean annual precipitation varies from 900 mm in the lowest parts of the region to 2000 mm and more in the highest sites. The average snow cover duration is more than 200 days in a year. The average mean monthly temperature in January ranges between –10 to –6° C and in July 11–15° C.

Precipitation regime in Slovakia is influenced predominantly by three main factors: 1) The *continental* one with maximum precipitation totals in June or July, when the best physical conditions for convective precipitation exists; and minimum precipitation totals in January to March, when the Siberian anticyclone blocks the Atlantic and Mediterranean factors, and low temperature causes low amount of water vapour in the atmosphere; 2) The *Atlantic* factor with equally distributed precipitation all year round, with some higher totals in the second half of the year (September to January) and some lower precipitation in the spring; 3) The *Mediterranean* factor, mainly due to Vb cyclonic situation occurrence; due to a blocking by the Siberian anticyclone, this influence is more pronounced in the autumn and spring in Slovakia.

Another important factor is connected with the regular summer shift of the European polar frontal zone to the north. This factor is partly modified by the positive or negative phase of the North-Atlantic oscillation. Mainly in northwestern Slovakia, there can be recognized an increase of precipitation totals from November to January in some years; such a phenomenon is typical for northwestern Europe.

The resulting precipitation patterns are rather complex at different Slovak stations (*Lapin and Tomlain, 2001; Lapin et al., 2001, Kriegerová and Kohnová, 2005*). Southern Slovakia is more influenced by the Mediterranean regime, while northeastern Slovakia by the continental one. Some upwind and lee localities have specific precipitation regime not occurring anywhere else in Slovakia (climatological stations such as Modra, Motyčky etc., *Lapin et al., 2001*).

In the Tatra Mountains especially, a further important factor needs to be taken into account. The atmospheric currents in this area are quite regular from the WSW in the cold season and from WNW in the warm season. That is why the Poprad Hollow and some eastern slopes of mountains have significantly lower precipitation totals due to lee effects, mainly in the convective precipitation free season (October to March, i.e. the cold season). On the other hand, the western and northwestern slopes have much higher totals in the same season. Fig. 2 shows long-term annual patterns of monthly precipitation totals at 5 stations in comparison with Hurbanovo (SW Slovakia) and the Slovakia average (based on 203 stations), all in the period 1901–

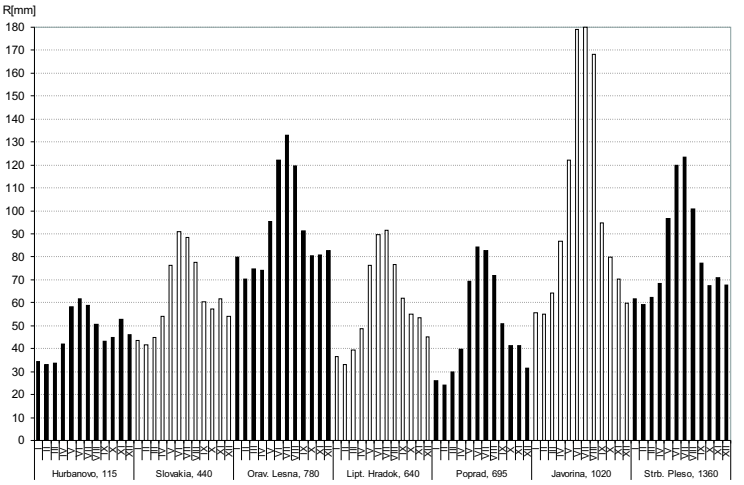

Fig. 2. Annual patterns of mean monthly precipitation totals at 5 stations around the High Tatras in the period 1901–2000 (Oravská Lesná, 780 m a.s.l., 100 km to NW; Liptovský Hrádok, 640 m a.s.l., hollow, 40 km to SW; Poprad, 695 m a.s.l., hollow, 25 km to SE; Javorina, 1020 m a.s.l., northern foot; Štrbské Pleso, 1360 m a.s.l., SW foot) in comparison with the Slovakia-wide average (440 m a.s.l., from 203 stations) and with Hurbanovo (115 m a.s.l., lowland, SW Slovakia).

2000. Precipitation regime in the warm season is dominantly influenced by convective events (thunderstorms, showers, cloudbursts). These are less determined here by the general atmospheric circulation currents and more by local conditions not clearly correlated with the altitude. Some sites are more impacted by summer heavy rains probably due to preferred tracks of convective clouds among mountains. The summer heavy rains connected with thunderstorms do not depend on altitude neither in other Slovak areas (*Šamaj and Valovič, 1973; Šamaj et al., 1985*).

5. Results

5.1. Identification of three homogeneous regions

Homogeneous regions for regional precipitation frequency analysis (*Hosking and Wallis, 1997*) in Slovakia have been delineated in three steps (*Gaál, 2006*):

1. In the firsts step, *cluster analysis* as an objective method of pooling has been carried out. Five discriminating variables have been selected: latitude, longitude, elevation, the ratio of the precipitation totals for the warm and cold seasons, and Lapin's index of the Mediterranean effect (the latter attribute is a special descriptor of the inter-annual variability of monthly precipitation totals in Slovakia; for further details, see *Gaál, 2005; Lapin and Melo, 2005*). The analysis resulted in a delineation of 5 homogeneous and geographically contiguous regions.
2. A *process-based* (subjective) regionalization has been proposed by Faško, one of the most experienced specialists on the long-term precipitation conditions of Slovakia (*Faško, 2006*). Taking into consideration the rich topography of the country and the effects of different patterns of general air-mass circulation, 4 regions of extreme precipitation have been identified.
3. The final set of regions for the RFA of heavy precipitation totals in Slovakia has been created as a *compromise between the results of the objective and the subjective methods* of regionalization, respectively. On one hand, there was an effort to preserve integrity of individual geographical units; on the other hand, one of the main goals was to

get as acceptable test statistics as possible. The final set of regions as a compromising solution of the problem consists of 3 regions (Fig. 3). Further considerations about how the regions were identified are given in *Gaál (2006)*.

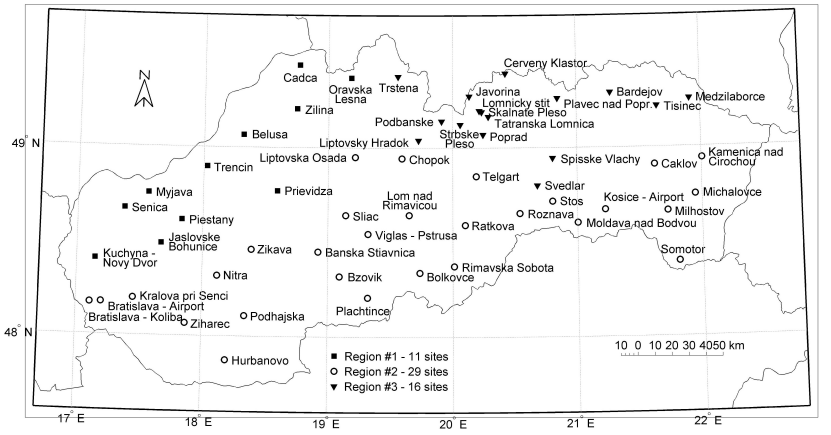

Fig. 3. Composition of three homogeneous regions for a frequency analysis of heavy precipitation totals in Slovakia.

5.2. Regional homogeneity of Region #3

Region #3 (Fig. 3) consists of 16 stations in the north of the country, including the whole High Tatras region (8 stations - Table 1). The group of sites is a mixture of high- and middle-elevated sites – the average (median) elevation is 828 m (622 m).

Even though Region #3 encompasses different geographical units of the country (the ridge of High Tatras with altitudes over 2000 m a.s.l., the Podtatranská basin between the High and Low Tatras, the Spiš basin with the most remarkable rainfall shadow effect of the Tatras mountain, and a hilly region with altitudes 3-500 m a.s.l. in the northeastern parts of the country), the most of the heterogeneity measures (Table 2) indicate homogeneity of the region. It holds particularly true for the cold season where the statistics of both tests are relatively far below the critical values; moreover, negative values of the H-test for the durations of 1 to 3 days indicate high

Table 1. Stations included in Region #3 for frequency analysis of heavy precipitation totals in Slovakia

Station ID	Station name	Latitude	Longitude	Elevation [m a.s.l.]	Included in the High Tatras region
11870	Trstená - Ústie nad Priehradou	49°23'	19°34'	604	-
11874	Liptovský Hrádok	49°02'	19°44'	640	✓
11876	Podbanské	49°08'	19°55'	972	✓
11930	Lomnický Štít	49°12'	20°13'	2635	✓
11931	Skalnaté Pleso	49°11'	20°14'	1783	✓
11933	Štrbské Pleso	49°07'	20°04'	1354	✓
11934	Poprad	49°04'	20°15'	695	✓
11935	Tatranská Lomnica	49°10'	20°17'	827	✓
11936	Ždiar - Javorina	49°16'	20°08'	1030	✓
11945	Švedlár	48°48'	20°41'	550	-
11949	Spišské Vlachy	48°57'	20°48'	380	-
11951	Červený Kláštor	49°24'	20°26'	465	-
11961	Plaveč nad Popradom	49°16'	20°51'	485	-
11962	Bardejov	49°17'	21°16'	305	-
11976	Stropkov - Tisinec	49°13'	21°39'	216	-
11977	Medzilaborce	49°15'	21°55'	305	-

Table 2. Results of the homogeneity tests for Region #3 (16 stations). The critical value of the *X10*-test is $\chi^2_{0.95,N-1} = \chi^2_{0.95,15} = 25.00$. Figures marked in bold indicate possible heterogeneity (*H*-test) or heterogeneity (*X10*-test)

Region #3 (16 stations)	Calendar year ($\chi^2_{0.95,15} = 25.00$)		Warm season ($\chi^2_{0.95,15} = 25.00$)		Cold season ($\chi^2_{0.95,15} = 25.00$)	
	H-test	*X10*-test	*H*-test	*X10*-test	*H*-test	*X10*-test
1-day prec. maxima	**1.66**	24.42	**1.23**	20.00	-1.11	13.91
2-day prec. maxima	0.99	22.73	0.93	19.98	-0.13	14.51
3-day prec. maxima	0.91	21.90	0.83	20.38	-0.13	18.32
4-day prec. maxima	0.46	19.23	0.41	18.08	0.00	17.43
5-day prec. maxima	**1.01**	22.54	0.66	19.87	0.05	18.50

degree of homogeneity, possibly due to an excessive regularity of the occurrence of precipitation extremes that results in cross-correlated structure of the data series. On the other hand, H values for the other seasons reveal more diverse view of the analyzed data sets. Some of H statistics yield possible heterogeneity (1D/WS, 1D/Year, 5D/Year), while other ones lie only slightly below the critical value of 1.0 (2D and 3D precipitation both for the warm season and calendar year).

A detailed scrutiny of the data sets revealed that the higher heterogeneity measures for the warm season and calendar year occur likely due to Podbanské station. The climatological station in Podbanské has a very specific location at the southeastern foot of the Western Tatras, which under certain synoptic situations enhances the formation of precipitation on the leeward sides of the surrounding slopes. In the period 1961-2003, four extraordinary daily precipitation totals exceeding 100 mm (126.9; 120.5; 112.2 and 105.4 mm) were recorded at the station; on the contrary, the fifth largest extreme did not reach the amount of 70 mm. These events cause a relatively skewed sample of the 1-day annual and the warm season maxima at Podbanské station that is clearly discernible at the L-moment ratio diagrams (Fig. 4) by the outlying position of the site's data in the top right corners of Figs. 4a) and 4c) (indicated by a bigger circle). The outstanding position of the station is still obvious in the case of 5-day durations (Figs. 4b) and 4d)); however, since the H-test is based on the L-Cv-s, the heterogeneity measures dropped compared to the 1-day duration. The last two diagrams (Figs. 4e) and 4f)) are aimed at demonstrating an ordinary behaviour of Podbanské station in the cold season: the more or less evenly scattered clouds of dots do not indicate regional heterogeneity. The L-moment ratio diagrams for the other combinations of durations (2 to 4 days) and three seasons reveal similar general features (not shown here).

A summary of the heterogeneity measures in the case of a hypothetical situation if the station Podbanské was excluded from Region #3 is given in Table 3. In this case, the heterogeneity measures, mostly for the shorter durations, would drop considerably. The only exception is the data set 5D/Year where practically no change is observed; however, the value 1.03 cannot still be considered as an indicator of heterogeneity. In general, Table 3 suggests that the remaining 15 stations would form a definitely homogeneous region regardless of the duration of the precipitation and the seasons of the year.

The High Tatras region, in strict sense, is formed by 8 stations – the test statistics confirm homogeneity of this sub-region (Table 4). The exclusion of the station Podbanské from the High Tatras region results, again, in a bit higher degree of homogeneity for the annual maxima and the ones in the warm season (Table 5).

According to the homogeneity analyses of regions of different composi-

tions it is very likely that the source of inhomogeneities in Region #3 is the station Podbanské. In principle, this 'problematic' station could be removed from Region #3; however, there are at least three reasons why not to do so:

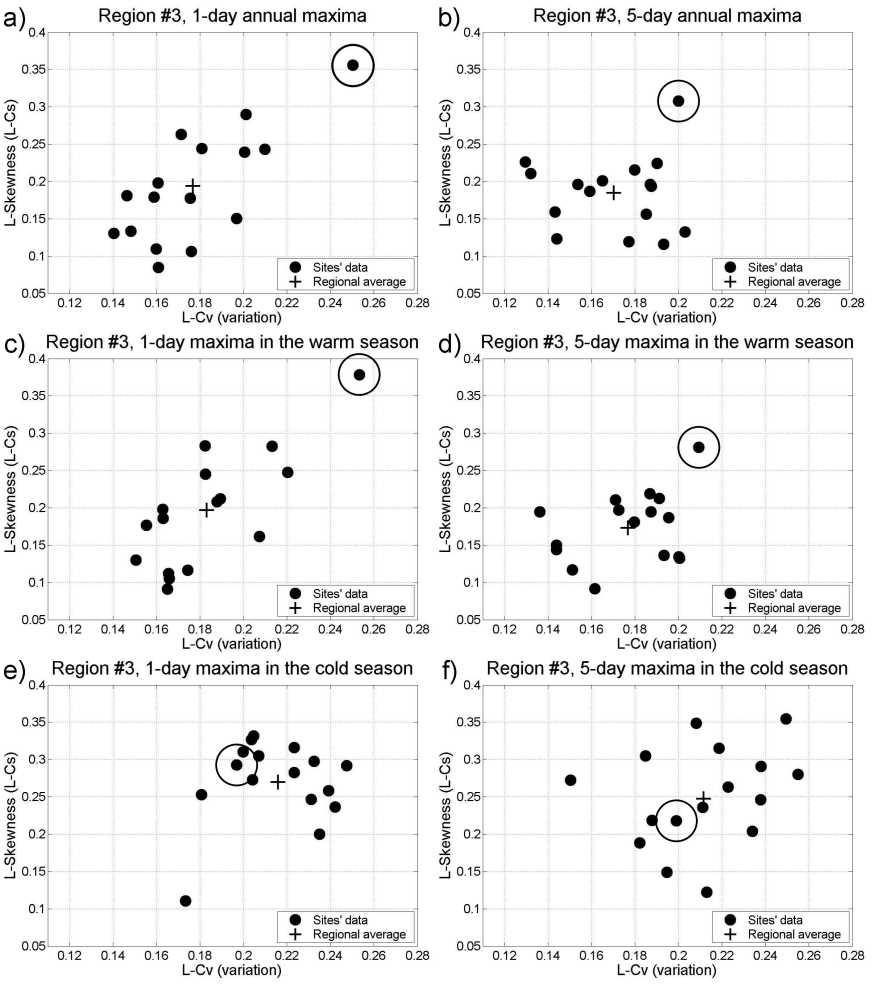

Fig. 4. L-moment diagrams (L-skewness vs. L-Cv) for selected durations (left side: 1 day; right side: 5 days) and three seasons for Region #3. The small, solid circles represent the at-site data, while the '+' sign is their weighted regional average. The position of Podbanské station is indicated by a larger circle.

Table 3. Results of the homogeneity tests for Region #3 with 15 stations after excluding the station Podbanské. The critical value of the *X10*-test is $\chi^2_{0.95,N-1} = \chi^2_{0.95,14} = 23.69$. Figures marked in bold indicate possible heterogeneity (*H*-test) or heterogeneity (*X10*-test)

Region #3 (15 stations)	Calendar year ($\chi^2_{0.95,14}$ = 23.69)		Warm season ($\chi^2_{0.95,14}$ = 23.69)		Cold season ($\chi^2_{0.95,14}$ = 23.69)	
	H-test	*X10-test*	*H-test*	*X10-test*	*H-test*	*X10-test*
1-day prec. maxima	0.27	16.52	-0.05	14.29	0.19	13.13
2-day prec. maxima	0.37	18.15	0.34	16.47	0.09	13.53
3-day prec. maxima	0.53	18.48	0.52	17.62	-0.02	18.17
4-day prec. maxima	0.21	16.69	0.23	16.00	-0.62	16.92
5-day prec. maxima	**1.03**	21.64	0.58	18.23	-1.08	18.24

Table 4. Results of the homogeneity tests for the High Tatras region (8 stations). The critical value of the *X10*-test is $\chi^2_{0.95,N-1} = \chi^2_{0.95,7} = 14.07$. Figures marked in bold indicate possible heterogeneity (*H*-test) or heterogeneity (*X10*-test)

High Tatras region (8 stations)	Calendar year ($\chi^2_{0.95,7}$ = 14.07)		Warm season ($\chi^2_{0.95,7}$ = 14.07)		Cold season ($\chi^2_{0.95,7}$ = 14.07)	
	H-test	*X10-test*	*H-test*	*X10-test*	*H-test*	*X10-test*
1-day prec. maxima	**1.04**	12.93	0.79	10.64	-0.61	7.40
2-day prec. maxima	0.05	7.08	0.36	7.15	-0.78	5.15
3-day prec. maxima	0.24	8.04	0.39	7,93	-0.12	8.37
4-day prec. maxima	-0.36	5.61	-0.15	5.89	0.24	9.63
5-day prec. maxima	-0.79	4.01	-0.75	4.06	-0.14	7.82

1. There could not be found a more suitable region where Podbanské station might be assigned to: it would surely increase the heterogeneity measures in any other regions.
2. There is no reason for excluding the station from the whole analysis, as a lot of valuable information about the precipitation extremes would be then lost.
3. One of the basic principles of regional approach says that even though a region is moderately heterogeneous, RFA will still yield much more accurate quantile estimates than at-site analysis (*Hosking and Wallis, 1997*).

Therefore, even though being an outlying one, the station Podbanské will be retained in the further analyses. What is more, although the High Tatras

region shows a slightly higher degree of homogeneity (Table 4) than Region #3 (Table 2), the estimation of design values at the stations of the High Tatras region will be based on the regional analysis within Region #3: the drawbacks originating from the possible heterogeneity of some data sets are supposed to be outweighed by the benefits from pooling information of the precipitation extremes from a wider region.

Table 5. Results of the homogeneity tests for the High Tatras region with 7 stations after excluding the station Podbanské. The critical value of the *X10*-test is $\chi^2_{0.95,N-1} = \chi^2_{0.95,6} = 12.59$. Figures marked in bold indicate possible heterogeneity (*H*-test) or heterogeneity (*X10*-test)

High Tatras region (7 stations)	Calendar year ($\chi^2_{0.95,6}$ = 12.59)		Warm season ($\chi^2_{0.95,6}$ = 12.59)		Cold season ($\chi^2_{0.95,6}$ = 12.59)	
	H-test	*X10-test*	*H-test*	*X10-test*	*H-test*	*X10-test*
1-day prec. maxima	0.11	7.71	-0.09	6.96	-0.55	6.10
2-day prec. maxima	-0.74	3.84	-0.38	4.53	-0.81	3.99
3-day prec. maxima	-0.18	5.54	0.08	6.08	0.04	8.16
4-day prec. maxima	-0.71	3.79	-0.30	4.76	0.39	9.06
5-day prec. maxima	-0.81	3.43	-0.86	3.26	0.01	7.30

5.3. Selecting a regional frequency distribution

The *Z*-test (Section 2.3.) by *Hosking and Wallis (1997)* has been applied to choose an appropriate regional frequency distribution. Algorithms for computing the goodness-of-fit statistics are included in the *Xtest.f* program that is a part of the package of freely available *Fortran* routines for RFA (*Hosking, 2000*).

For each data set, fitting of the following 3-parameter DFs to the observed data has been tested:

- GEV - generalized extreme value,
- GLO - generalized logistic,
- GNO - generalized normal,
- PE3 - Pearson type III.

Note that even though the generalized Pareto (GPA) distribution is also included in the software package of *Hosking (2000)*, we ignored it due to

Table 6. Results of the goodness-of-fit test by *Hosking and Wallis (1997)* for Region #3: a summary of the Z-statistics as the acceptability of the distribution functions. Abbreviations of the distribution functions: GEV – generalized extreme value; GNO – generalized normal; PE3 – Pearson type III; GLO – generalized logistic. Symbols: $-/+/\oplus$ – not suitable / acceptable / accepted distribution function. Z-values for the acceptable distributions are also indicated in bold

Region #3 (16 stations)	Calendar year				Warm season				Cold season			
	GEV	GNO	PE3	GLO	GEV	GNO	PE3	GLO	GEV	GNO	PE3	GLO
1-day prec. maxima	**-0.38**	**-0.91**	-2.05	2.17	**-0.45**	**-1.02**	-2.22	2.12	**-0.97**	-1.91	-3.56	**0.64**
	⊕	+	–	–	⊕	+	–	–	⊕	–	–	+
2-day prec. maxima	**-0.27**	**-0.76**	-1.88	2.37	**0.18**	**-0.29**	**-1.41**	3.04	**-1.23**	-2.01	-3.45	**0.65**
	⊕	+	–	–	⊕	+	+	–	⊕	–	–	+
3-day prec. maxima	**0.01**	**-0.42**	**-1.49**	2.80	**-0.08**	**-0.37**	**-1.31**	3.07	**-1.30**	-2.19	-3.77	**0.33**
	⊕	+	+	–	⊕	+	+	–	⊕	–	–	+
4-day prec. maxima	**-0.10**	**-0.53**	**-1.58**	2.69	**0.12**	**-0.26**	**-1.29**	3.14	**-0.80**	**-1.62**	-3.10	**1.12**
	⊕	+	+	–	⊕	+	+	–	⊕	+	–	+
5-day prec. maxima	**0.17**	**-0.30**	**-1.41**	2.92	**-0.14**	**-0.52**	**-1.54**	2.84	**-0.60**	**-1.45**	-2.99	**1.28**
	⊕	+	+	–	⊕	+	+	–	⊕	+	–	+

the very poor fit in all the cases (in fact, GPA is rather suitable for the data selected according to the peaks-over-threshold method; *Madsen et al., 1997*). In the case when none of the 3-parameter distribution functions is acceptable, it is advised to fit the 4-parameter Kappa or the 5-parameter Wakeby distribution (*Hosking and Wallis, 1997*).

The results of the goodness-of-fit tests are summarized in Table 6. It shows that the GEV distribution is acceptable for each data set. Differences appear at looking at the seasons separately: while the DF GNO is generally suitable for the calendar year and the warm season, GLO is acceptable for each duration in the cold season.

L-moment ratio diagrams (L-Cs vs. L-Ck) usually serve for evaluating the goodness of fit of the DFs to the given data in a subjective way. Fig. 5 displays L-moment ratio diagrams for selected data sets of Region #3. In each case, the '+' sign that indicates the centroid of the cloud of dots lies between the GLO and the GEV DFs. In the most cases, however, the '+'; mark is placed approximately half way between the two adjacent curves of the candidate DFs, therefore it is hard to draw clear conclusions about which one is the most suitable distribution function to fit. Note that the L-moment ratio diagrams and the Z-test carry similar but slightly different information: at both of them, the key role is assigned to the difference

$\tau_4^{DF} - t_4^R$; however, the Z-test also involves two more statistics B_4 and σ_4 (Eq. 9).

In the end, we chose the GEV distribution as the regional distribution function for all the data sets in Region #3 ($\oplus$ signs in Table 6). The

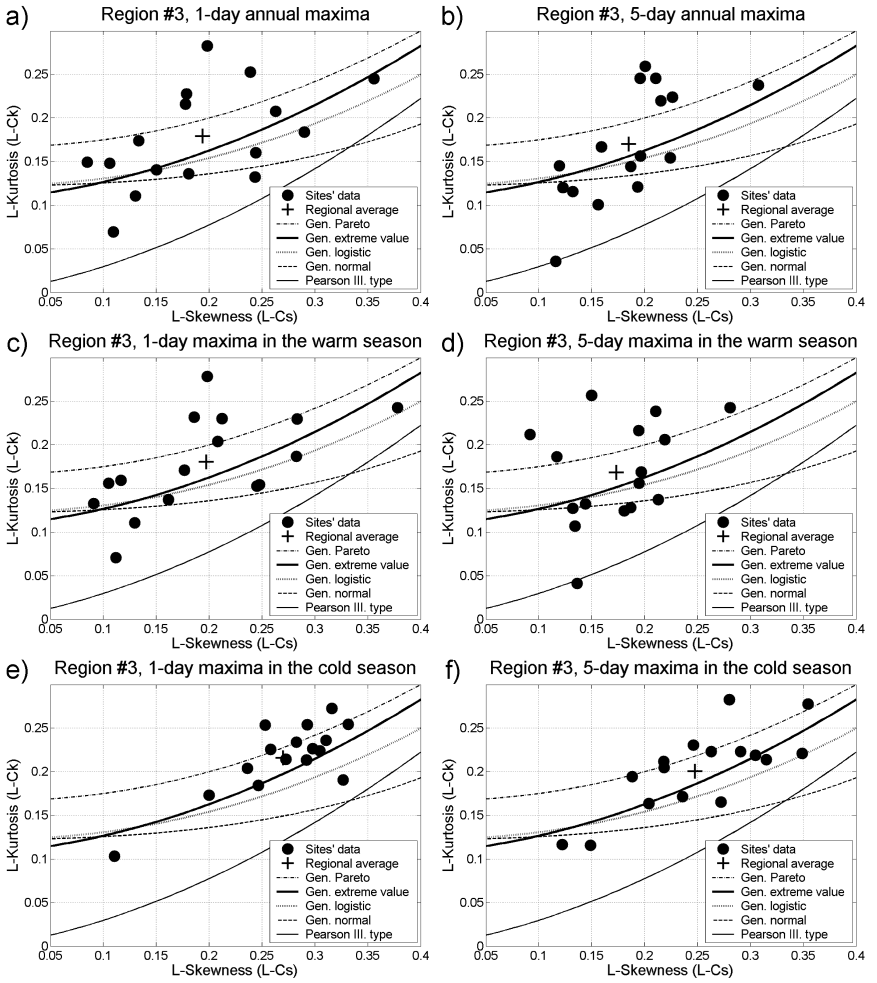

Fig. 5. L-moment diagrams (L-kurtosis vs. L-skewness) for selected durations (left side: 1 day; right side: 5 days) and three seasons for Region #3. The small, solid circles represent the at-site data, while the '+' sign is their weighted regional average.

GEV DF has been selected mainly according to the principles of the robustness: it says that the frequency model should yield quantile estimates whose accuracy is not seriously degraded when the true physical process deviates from the model's assumption in a plausible way (*Hosking and Wallis, 1997*). The principle of robustness may be interpreted also in the way that if there exist more DFs acceptable for the given data set, the *accepted* DF does not necessarily need to be the one with the Z-value closest to zero. Instead, more important aspect is a consistency between the selected DFs when moving from one duration to another. For example, the cold-season precipitation maxima of the durations 3 and 4 days are supposed to have similar statistical properties due to negligible differences in mechanisms of their generation (predominantly of frontal origin). Therefore, there is no particular reason why to fit, strictly according to the smallest $|Z|$-values in Table 6, a rather heavy-tailed GLO DF to the data 3D/CS, and the considerably different GEV DF to the data 4D/CS. The GEV distribution has therefore been selected for all the durations in the cold season. Moreover, an overall goodness-of-fit of the GEV DF has been confirmed in the case of the majority of the data sets within the other two regions in Slovakia (not shown here).

5.4. Regional growth curves for Region #3

Figs. 6a), c) and e) show the dimensionless regional growth curves for Region #3, where growth curves corresponding to durations $k = 1$ to 5 days in a given season are clustered together. Their general features may be summarized as follows:

- *Growth curves often overlap.* Individual growth curves are discernible practically from return period $T \sim 50$ years up. Considerable distances between different curves become apparent only when the actual quantile functions of the individual stations (i.e. the regional growth curves multiplied by the at-site index value, Eq. 1) are displayed (not shown here).

- *The order of the growth curves is sometimes mixed.* The slope (curvature) of the growth curves is in close relationship with the skewness

(kurtosis) of the sample. In an ideal case, when the region is homogeneous, and there are no extraordinary precipitation totals that would increase the regional average of the L-Cs and/or L-Ck, the growth

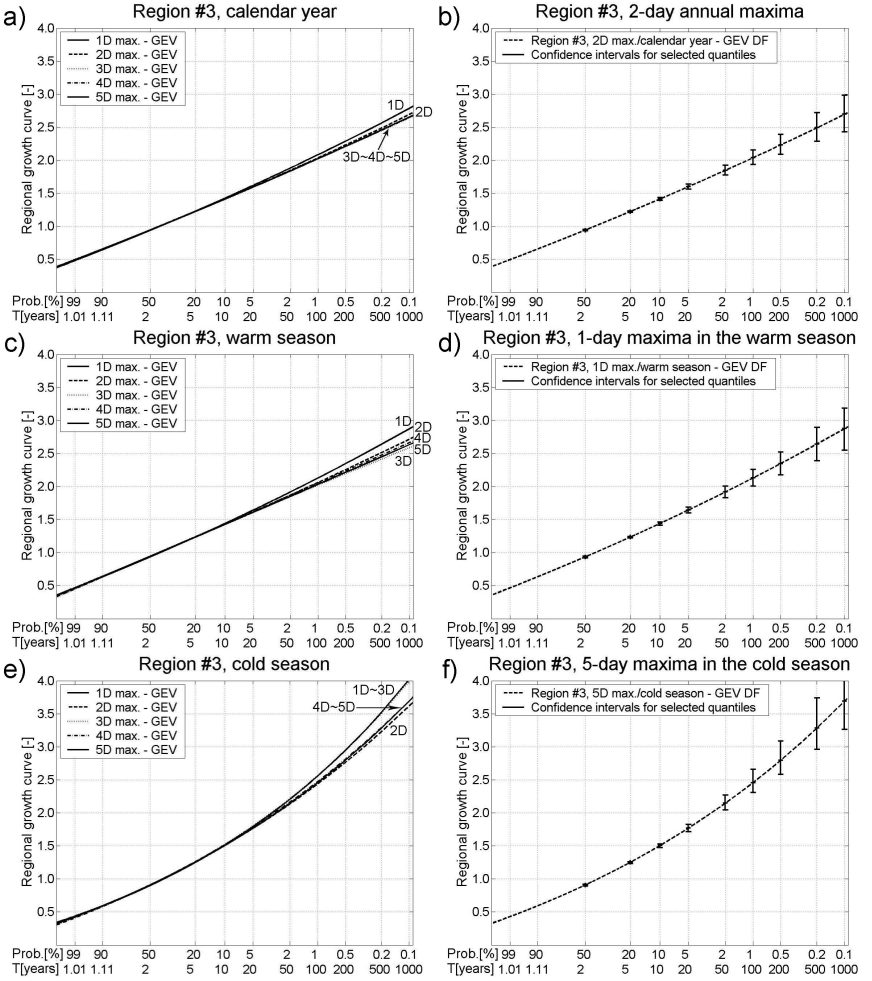

Fig. 6. Dimensionless regional growth curves for Region #3. On the left side: for a given season, growth curves corresponding to 1 to 5-day durations clustered together. On the right side: for a given season, a growth curve corresponding to a selected duration displayed together with its 90% confidence bounds.

curves for different durations k are arranged successively one below the other (i.e. the longer the duration k, the lower the slope of the growth curve). Growth curves for the annual maxima (Fig. 6a) are relatively close to this ideal situation, at least in rough estimation. On the other hand, due to enhanced sample variability, a mixed arrangement of the growth curves can be seen for the cold season (Fig. 6e).

The accuracy of growth curve quantiles have been assessed by means of the properly modified Fortran routine *Xsim.f* that is a part of the *Hosking's (2000)* package of codes for the RFA. Selected regional growth curves along with the 90% confidence intervals of some quantiles are shown on Figs. 6b), d) and f). Error bounds have only been determined for quantiles corresponding to significant return periods ranging from $T = 2$ years to 1000 years; however, the quantiles for the longest return periods ($T = 500$ and 1000 years) serve purely as illustration: their values are not considered in evaluation of the analysis. We only display confidence intervals for one selected data set for each season as the growth curves and their error bounds are rather similar for different durations within a given season (cf. Table 7).

A numerical evaluation of the confidence intervals of the growth curves has been assessed by the relative error RE of the quantile estimates. Considering Eqs. 12–13, the expression for the relative error reduces into a very simple form:

$$RE_T = \frac{u_T - l_T}{q_T} = k_{0.95,\,T} - k_{0.05,\,T}. \tag{14}$$

RE_T values are summarized in Table 7, where the following properties can be noticed:

- The widths of the confidence intervals are rather similar for different durations k within the same season and for the same return period.
- There are no clear rules, likely due to the sampling variability, for the dependence of RE_T on k.
- The width of the confidence intervals depends on the return period of the estimated quantiles: naturally, the longer the return period (the less the probability of occurrence of the event), the higher the uncertainty in the estimation of the quantiles (the higher the value RE_T) – and vice versa.

Table 7. Relative error RE [%] of the regional growth curve estimates corresponding to return periods $T = 2$ to 200 years in Region #3

Region #3		T [years]						
		2	5	10	20	50	100	200
Calendar year	1-day prec. maxima	2.5	1.8	3.2	5.3	8.6	11.5	14.4
	2-day prec. maxima	2.3	1.8	3.0	4.9	8.1	10.7	13.5
	3-day prec. maxima	2.3	1.8	2.9	4.8	7.9	10.4	13.1
	4-day prec. maxima	2.3	1.8	2.9	4.8	7.9	10.5	13.2
	5-day prec. maxima	2.3	1.8	3.0	4.9	8.0	10.6	13.4
Warm season	1-day prec. maxima	2.6	1.9	3.2	5.4	8.9	11.8	14.8
	2-day prec. maxima	2.3	1.9	3.1	5.0	8.2	10.8	13.6
	3-day prec. maxima	2.3	1.9	3.0	4.8	7.7	10.1	12.6
	4-day prec. maxima	2.3	1.9	3.0	4.9	8.0	10.5	13.1
	5-day prec. maxima	2.3	1.9	3.0	4.9	7.9	10.4	13.1
Cold season	1-day prec. maxima	3.6	2.0	3.5	6.4	11.1	15.1	19.4
	2-day prec. maxima	3.3	2.0	3.5	6.1	10.4	13.9	17.7
	3-day prec. maxima	3.5	2.1	3.6	6.5	11.1	15.1	19.4
	4-day prec. maxima	3.3	2.0	3.5	6.2	10.5	14.1	18.1
	5-day prec. maxima	3.3	2.0	3.5	6.2	10.5	14.2	18.2

Obviously, the statements above hold true only for the case where the same DF is selected for all the durations within the same season and the region, respectively. RE_T depends on the DF selected – for instance, the DF GLO with a heavy tail has wider error bounds than the other 3-parameter distribution functions selected for the same data set (not shown here). Furthermore, RE_T depends on the size of the region (i.e. higher number of sites in a region provides higher amount of information that may reduce the uncertainty in the quantile estimates); nevertheless, such a conclusion cannot be proven based only on Region #3.

6. Summary and conclusions

The main steps to be conduced in modern regional frequency analysis, namely the identification of homogeneous regions, testing their spatial homogeneity, and the choice and estimation of the regional frequency distribution function, were presented in a case study which focuses on the

description of the regime of extreme precipitation of the High Core Mountain region of Slovakia. The analysis has been performed on maxima of one to five-day precipitation totals in the warm and cold seasons and on annual basis.

Alternatives of a subjective, process-based regionalization and objective regionalization were considered. In all cases, homogeneous, as well as possible or definitively heterogeneous regions have been identified by independent homogeneity tests. An often observed feature of such homogeneity testing, that inhomogeneities are usually caused by the same stations across various regionalization schemes, was observed. In such a case, it is sometimes difficult to allocate such stations into an appropriate region in which they would not destroy the regional homogeneity. In the case of the High Core Mountains and their surroundings the station Podbanské was identified as suspicious in this respect. It was beyond the scope of this study to find detailed reasons for such a behavior, only few possibilities were given in the text above.

The design precipitation values estimated in course of the analysis in the paper can be used for the purposes described in the introduction of the paper and for conventional engineering design (e.g. *Kohnová, 1998*). Further recommendations and conclusions, with emphasis on the applicability of regional frequency analysis in engineering analyses, may be summarized as follows. If one is interested in calculating design values at a given site with return periods T shorter than the length of the observation n, the estimation may be based both on regional as well as on at-site approach. Nevertheless, it is strongly advised to use regional methods if one desires to extrapolate the return periods T beyond the length of the available data series n.

The delineation of regions is always biased by subjective reasoning, regardless if logical, process-based, or mathematical methods are applied. In the case of the latter, though the selection of the stations belonging into a group is based on an objective process (e.g. cluster analysis), the selection of the discriminating variables is made by the analyst lead by his views and experience. It has to be noted, that no unique choice of a set of discriminating physiographic characteristics can be made. Therefore, the use of the combination of objective and subjective regionalization, which was suggested as an option in the paper, can be seen as justifiable.

However, regardless of the way of delineating the regions, the information gathered from sites of a given region favorably reduces the uncertainty of the estimated quantiles in comparison to at-site estimates (*Hosking and Wallis, 1997*). It is obvious that the magnitude of the uncertainty of a design value is also dependent on the composition of the regions. In order to determine the most suitable delineation of regions (and, in a broader sense, the most acceptable regional frequency model), it is necessary to get information about the spread of the estimates as well, for example by means of multiple Monte Carlo simulations. Such an analysis was beyond the scope of this study.

Acknowledgments. The work was supported under the HYDRATE project, Contract GOCE 037024, and the project 1/4024/07 of the Slovak VEGA Grant Agency. The authors would like to thank the Slovak Hydrometeorological Institute for providing the precipitation data.

References

Borga M., 2002: Accuracy of radar rainfall estimates for streamflow simulation. Journal of Hydrology, **267**, 26–39.

Coles S., 2001: An introduction to statistical modeling of extreme values. Springer-Verlag, London, 222 p.

Dalrymple T., 1960: Flood frequency analyses. Water Supply Paper 1543-A. U. S. Geological Survey, Reston.

Delrieu G., Ducrocq V., Gaume E., Nicol J., Payrastre O., Yates E., Kirstetter P. E., Andrieu H., Ayral P. A., Bouvier C., Creutin J. D., Livet M., Anquetin S., Lang M., Neppel L., Obled C., Parent-duChatelet J., Saulnier G. M., Walpersdorf A., Wobrock W., 2005: The catastrophic flash-flood event of 8–9 September 2002 in the Gard region, France: a first case study for the Cévennes-Vivarais Mediterranean Hydro-meteorological Observatory. Journal of Hydrometeorology, **6**, 1, 34–52.

Faško P., 2006: Slovak Hydrometeorological Institute. March, 2006. Personal communication, pavol.fasko@shmu.sk.

Fill H. D., Stedinger J. R., 1995: Homogeneity test based upon Gumbel distribution and a critical appraisal of Dalrymple's test. Journal of Hydrology, **166**, 1–2, 81–105.

Gaál L., 2005: Introduction of Lapin's indices into the cluster analysis of maximum k-day precipitation totals in Slovakia. Meteorological Journal, **8**, 2, 85–94.

Gaál L., 2006: Estimation methods of statistical properties of short-term to several-day design precipitation in Slovakia. Ph.D. thesis, Faculty of Mathematics, Physics and Informatics, Comenius University in Bratislava. 228 p. (in Slovak).

Gaume E., Livet M., Desbordes M., Villeneuve J. P., 2004: Hydrological analysis of the river Aude, France, flash flood on 12 and 13 November 1999. Journal of Hydrology, **286**, 1, 135–154.

Hlavčová K., Kohnová S., Kubeš R., Szolgay J., Zvolenský M., 2005: An empirical method for estimating future flood risk for flood warnings. Hydrology and Earth System Sciences, **9**, 4, 431–488.

Hosking J. R. M., 1990: *L*-moments: analysis and estimation of distributions using linear combinations of order statistics. Journal of the Royal Statistical Society, Series B, **52**, 1, 105–124.

Hosking J. R. M., 2000: Fortran routines for use with the method of *L*-moments – Version 3.03. Research Report RC 20525. IBM Research Division, Yorktown Heights, NY, USA, 33 p.

Hosking J. R. M., Wallis J. R., 1997: Regional frequency analysis: an approach based on *L*-moments. Cambridge University Press, Cambridge, 224 p.

Kohnová S., 1998: Regional analysis of maximum seasonal specific discharges on small and mid-sized catchments in Slovakia. Slovak Journal of Civil Engineering, Vol. VI, **4**, 27–34.

Kriegerová I., Kohnová S., 2005: Seasonality analysiss of flood occurence in mid-sized catchments in Slovakia. Journal of Hydrology and Hydromechanics, **53**, 3, 154–163.

Lapin M., Tomlain J., 2001: General and regional climatology. Comenius University, Bratislava, Slovakia, 184 p. (in Slovak).

Lapin M., Damborská I., Melo M., 2001: Downscaling of GCM outputs for precipitation time series in Slovakia. Meteorological Journal, **4**, 3, 29–40.

Lapin M., Melo M., 2005: Spatial interpretation of climate scenarios' outputs in catchments of Hron and Váh rivers by means of geostatistical methods. In: Pekárová P. et al., 2005: Scenarios of selected components of the hydrosphere and biosphere in catchments of Hron and Váh rivers due to climatic change. VEDA, Bratislava, 49–80 (in Slovak).

Lu L.-H., Stedinger J. R., 1992: Sampling variance of normalized GEV/PWM quantile estimators and a regional homogeneity test. Journal of Hydrology, **138**, 1-2, 223–245.

Madsen H., Rasmussen P. F., Rosbjerg D., 1997: Comparison of annual maximum series and partial duration series methods for modeling extreme hydrologic events: 1. At-site modeling. Water Resources Research, **33**, 4, 747–757.

Norbiato D., Borga M., Sangati M., Zanon M., 2007: Regional frequency analysis of extreme precipitation in the eastern Italian Alps and the August 29, 2003 flash flood. Journal of Hydrology, **345**, 149–166.

Ramos M. H., Creutin J. D., Leblois E., 2005: Visualization of storm severity. Journal of Hydrology, **315**, 295–307.

Šamaj F., Valovič Š., Brázdil R., 1985: Daily precipitation totals with extraordinary substantiality in Czechoslovakia in 1901-1980. In: Proceedings of Works of the Slovak Hydrometeorological Institute, Alfa, Bratislava, **24**, 9–113 (in Slovak).

Šamaj F., Valovič Š., 1973: Intensities of short-term rains in Slovakia. Proceedings of Works of the Hydrometeorological Institute Bratislava. SPN, Bratislava, 93 p. (in Slovak).

Sankarasubramanian A., Srinivasan K., 1999: Investigation and comparison of sampling properties of L-moments and conventional moments. Journal of Hydrology, **218**, 1-2, 13–34.

Vogel R. M., Fenessey N. M., 1993: L-moments diagrams should replace product moment diagrams. Water Resources Research, **29**, 6, 1745–1752.

Wallis J. R., Schaefer M. G., Barker B. L., Taylor G. H., 2007: Regional precipitation-frequency analysis and spatial mapping for 24-hour and 2-hour durations for Washington State. Hydrology and Earth System Sciences, **11**, 1, 415–442.

Wilks D., 1995: Statistical methods in the atmospheric sciences. Academic Press, San Diego. 467 p.